Theoretical calculations of positron annihilation with rare-gas core electrons in simple and transition metals

S. Daniuk
W. Trzebiatowski Institute of Low Temperature and Structure Research, Polish Academy of Sciences, P.O. Box 937, PL-50-950 Wrocław 2, Poland

M. Šob
Institute of Physical Metallurgy, Czechoslovak Academy of Sciences, Žižkova 22, CS-616 62 Brno, Czechoslovakia

A. Rubaszek
W. Trzebiatowski Institute of Low Temperature and Structure Research, Polish Academy of Sciences, P.O. Box 937, PL-50-950 Wrocław 2, Poland
(Received 20 August 1990)

Positron-annihilation rates, momentum densities of positron-annihilation pairs, and electron-positron enhancement factors for rare-gas core electrons in 27 frequently investigated metals are calculated. The sensitivity of these quantities to various parameters of electron and positron models applied—namely, to the electron-electron exchange and correlation potential, electron configuration, lattice dimensions, and the shape of positron wave function, as well as the size of relativistic effects—is studied. The influence of inclusion of electron-positron correlations into both electron and positron wave functions on resulting annihilation characteristics is discussed. It is shown that the present approach reproduces fairly well also the total positron-annihilation rates and positron lifetimes.

I. INTRODUCTION

Angular correlation of positron-annihilation radiation (ACPAR) is a sensitive probe of electron and positron distributions in solids.[1] To obtain correctly the valence- or itinerant-electron part of the ACPAR spectrum, which is usually the main object of interest in electronic-structure studies, the subtraction of rare-gas core contribution must be, however, performed in a proper way. The usual approximation of this core part by the Gaussian component of the experimental ACPAR curve is, as a rule, not satisfactory.[2] Although some experimental[3,4] and theoretical[5–7] investigations of the core annihilation have already been done, further studies in this direction are necessary.

Because of the influence of positron wave function and of the many-body electron-positron (e^--e^+) correlations, the measured momentum distribution (MD) of annihilation pairs (AP's) differs from the electron momentum density, which is an important characteristic of the electronic structure in the material investigated. An exact inclusion of the electron-positron interaction into the calculations of MDAP's in real solids is, however, very difficult. Therefore, to interpret experimental data, one often combines the MDAP calculated within the independent-particle model (IPM) with theoretical or semiempirical enhancement factors (EF's), which take into account the e^--e^+ correlation effects (for a review, see, e.g., Refs. 1 and 8, and references therein).

Regrettably, there is not very much information about the EF's for ionic core electrons. By comparison of theoretical and experimental results, average values of core EF's in the low-momentum region ($p \leq 15$–20 mrad) were obtained and those for the high-momentum region ($p \geq 20$ mrad) were calculated[2] for a number of metals. It turns out that at the beginning of each series of metals Na–Al ($Z=11,12,13$) K–Zn ($Z=19$–30), and Rb-Cd ($Z=37$–48), there is a huge difference between the average EF in high- and low-momentum regions, whereas at the end of each series the difference in both averages is much smaller. Thus the constant core EF is an acceptable approximation in Al (Ref. 9) or Cu (Ref. 10), but fully unsatisfactory is alkali metals.[3] The momentum dependence of core EF's calculated in Ref. 7 in alkali metals and some simple metals is consistent with the average values of EF's in low- and high- momentum regions following from the analysis in Ref. 2. The averages of core EF's were determined also by Jensen,[6] without, however, predicting their momentum dependence. Those results were in good agreement with the low-momentum averages of Ref. 2 as well.

The purpose of the present paper is to show that the rare-gas core positron-annihilation characteristics are considerably sensitive to various details of the electron and positron models, similarly as the high-momentum components of valence momentum densities.[11] We determine the rare-gas core MDAP's and EF's in 27 frequently investigated metals, using different approaches to the

calculation of the electron and positron wave functions. To our knowledge these aspects of positron annihilation with rare-gas core electrons in metals are systematically analyzed for the first time.

After summarizing necessary theoretical formulas (Sec. II), the influence of the shape of positron wave function, electron-electron exchange and correlation potentials, electron configuration, relativistic effects, and change in lattice volume is investigated in Sec. III. Section IV is devoted to the study of the effect of the inclusion of electron-positron correlations into both the positron and electron wave functions. Section V summarizes the results and concludes the paper.

II. THEORETICAL BACKGROUND

The MDAP is given by the expression

$$\rho(\mathbf{p})=\sum_i \left| \int d\mathbf{r}\, e^{-i\mathbf{p}\cdot\mathbf{r}} \psi_i^{e^-e^+}(\mathbf{r},\mathbf{r}) \right|^2 , \tag{1}$$

where $\mathbf{p}$ is the photon-pair momentum and $\psi_i^{e^-e^+}(\mathbf{r}_e,\mathbf{r}_p)$ denotes the pair wave function of a thermalized positron at $\mathbf{r}_p$ and an electron in the initial state i located at $\mathbf{r}_e$. The total annihilation rate λ ($\lambda=1/\tau$, where τ is the positron lifetime) is given by

$$\lambda=\frac{\pi r_0^2 c}{(2\pi)^3}\int d\mathbf{p}\,\rho(\mathbf{p}) = \pi r_0^2 c \int d\mathbf{r} \left[\sum_i |\psi_i^{e^-e^+}(\mathbf{r},\mathbf{r})|^2 \right] , \tag{2}$$

where r_0 and c denote the classical electron radius and velocity of light, respectively. The summation in (1) and (2) runs over all occupied electronic states i. The core [$\rho_c(\mathbf{p})$ and λ_c] and valence [$\rho_v(\mathbf{p})$ and λ_v] parts of the MDAP and annihilation rate can be separated by dividing the summation in (1) and (2) over the core $\{i_c=(n,l,m)\}$ and valence $\{i_v=(\mathbf{k},j)\}$ electronic states, respectively (here n, l, and m are the usual atomic quantum numbers, and $\mathbf{k}$ and j are the Bloch wave vector and the band index).

The pair wave functions $\psi_i^{e^-e^+}(\mathbf{r},\mathbf{r})$ may be expressed by means of electron wave functions in the unperturbed system, $\psi_i^0(\mathbf{r})$, unperturbed positron wave function $\psi_+^0(\mathbf{r})$, and electron-positron correlation functions $g(\mathbf{r},i)$ in the following manner:

$$\psi_i^{e^-e^+}(\mathbf{r},\mathbf{r})=\psi_i^0(\mathbf{r})\psi_+^0(\mathbf{r})\sqrt{g(\mathbf{r},i)} . \tag{3}$$

The functions $g(\mathbf{r},i)$ describe both the distortion of the positron wave function from its initial shape ψ_+^0 and the enhancement of the densities of individual electronic states i on the positron site. The form of correlation functions g is related to the electronic screening charge distribution in the vicinity of a positron, $\Delta n(\mathbf{r}_{e^-},\mathbf{r}_{e^+})$. It should be noted here that the *pair*-correlation functions $g(\mathbf{r},i)$ defined in Eq. (3) are not the standard ones of density-functional theory (DFT). The present $g(\mathbf{r},i)$ describe the distortion of *individual* electron-positron wave functions $\psi_i^{e^-e^+}(\mathbf{r},\mathbf{r})$ from their values in the noninteracting system, $\psi_i^0(\mathbf{r})\psi_+^0(\mathbf{r})$, while the DFT correlation functions provide information about the perturbation of the *total* electron density, Δn, due to inclusion of interaction λV, where $\lambda\in[0,1]$ is an interaction parameter. The differences between the present two-particle $g(\mathbf{r},i)$ and usual DFT correlation functions are similar as between two-particle EF's and EF's of MDAP's discussed in the further part of this section.

As follows from Eqs. (1) and (2), total and partial (core, valence) MDAP's and annihilation rates are strongly dependent on the correlation functions $g(\mathbf{r},i)$. A proper determination of these functions in real metals is a complicated many-body problem, which is not completely solved yet.[12–14] Thus, in theoretical calculations, various approximations to $g(\mathbf{r},i)$ were applied.

The IPM, neglecting electron-positron correlations at all, i.e., assuming $g(\mathbf{r},i)\equiv 1$ [or, equivalently, $\Delta n(\mathbf{r}_{e^-},\mathbf{r}_{e^+})\equiv 0$], is the simplest of them, Within IPM Eqs. (1) and (2) reduce to the well-known expressions[1]

$$\rho^{\mathrm{IPM}}(\mathbf{p})=\sum_i \left| \int d\mathbf{r}\, e^{-i\mathbf{p}\cdot\mathbf{r}} \psi_i^0(\mathbf{r})\psi_+^0(\mathbf{r}) \right|^2 , \tag{1'}$$

and

$$\lambda^{\mathrm{IPM}}=\pi r_0^2 c \int d\mathbf{r}\, |\psi_+^0(\mathbf{r})|^2 \left[\sum_i |\psi_i^0(\mathbf{r})|^2 \right] . \tag{2'}$$

It turns out that the IPM reflects the main features of the MDAP reasonably well. Thus it is a good starting point for investigations of some positron-annihilation characteristics. A further step is an approximative inclusion of the e^--e^+ correlations into the calculation of the MDAP. Here attention was mainly focused on the valence electrons. The approaches used may be, in general, divided into two groups: the average electron density (AED) ones,[1,2,5,8,10,15,16] neglecting the $\mathbf{r}$ dependence of $g(\mathbf{r};\mathbf{k},j)$, and local ones,[6,7,17–20] taking into account the position dependence of $g(\mathbf{r};\mathbf{k},j)$ through local electron density in the absence of the positron $n(\mathbf{r})$. The mixed density approximation, used in Ref. 19 for calculations of MDAP's for positrons trapped at vacancies and metal surfaces, neglects the $(\mathbf{k},j)$ dependence of $g(\mathbf{r};\mathbf{k},j)$ and assumes the electron wave functions $\psi_{\mathbf{k}j}^0(\mathbf{r})$ in the form of plane waves. For the last reason this approach cannot be applied to determining of the MDAP of strongly localized core electrons. The formalism of Ref. 6, based on the total electron density, allows one to obtain total and partial annihilation rates only [according to the formula (2)] and could not lead to a MDAP which requires individual electron wave functions [cf. Eqs. (1) and (3) as well as the discussion in Ref. 20].

Special attention should be paid to the AED approach of Refs. 15, 10, and 16, which allows one to enhance the contributions of individual electronic states differently. In the present terms, the correlation function $g(\mathbf{r};\mathbf{k},j)$ corresponding to that approach may be written in the form

$$g(\mathbf{r};\mathbf{k},j)=\epsilon(X_{\mathbf{k}j},r_s) , \tag{4}$$

where $X_{\mathbf{k}j}=\sqrt{E_{\mathbf{k}j}/E_F}$, $E_{\mathbf{k}j}$ denotes the energy of the electronic state $(\mathbf{k},j)$, and E_F and r_s are Fermi energy

and electron-density parameter in the investigated material, respectively (both $E_{\mathbf{k}j}$ and E_F are counted from the bottom of conduction band). The quantities $\epsilon(p,r_s)$ represent the jellium-model two-particle momentum-dependent EF's in the biquadratic Kahana form.[21] This formalism was further developed by Daniuk *et al.*[17] and Jarlborg and Singh[18] into a local-density approach (LDA) and was just recently applied to calculation of core MDAP's and EF's in alkali metals and some simple metals.[7] In Refs. 7 and 17 the mean electron-density parameter r_s used in Eq. (4) was replaced by its local value $r_s(\mathbf{r})=[4\pi n(\mathbf{r})/3]^{-1/3}$. The correlation function used in Ref. 17 was thus of the form

$$g(\mathbf{r};\mathbf{k},j)=\epsilon[X_{\mathbf{k}j},r_s(\mathbf{r})] , \tag{5a}$$

employing the momentum-dependent two-particle EF's $\epsilon(p,r_s)$ calculated within the model of jellium for various electron-density parameters r_s.[13] Since the energies of the rare-gas core electronic states lie deeply below the bottom of the conduction band, the energy parameters for core states, X_{nlm}, were set equal to zero in Ref. 7. Thus the electron-positron wave function in the (n,l,m) ionic core shell was approximated by

$$\psi^{e^-e^+}_{nlm}(\mathbf{r},\mathbf{r})=\psi^0_{nlm}(\mathbf{r})\psi^0_+(\mathbf{r})\sqrt{\epsilon[0,r_s(\mathbf{r})]} . \tag{5b}$$

Let us note here that the usual EF's of valence or core MDAP's, defined as

$$\tilde{\epsilon}_v(\mathbf{p})=\rho_v(\mathbf{p})/\rho_v^{\mathrm{IPM}}(\mathbf{p}) , \tag{6a}$$

and

$$\tilde{\epsilon}_c(\mathbf{p})=\rho_c(\mathbf{p})/\rho_c^{\mathrm{IPM}}(\mathbf{p}) , \tag{6b}$$

respectively, are often identified with the two-particle parameters $\epsilon(X_i=p,\ r_s)$ (Refs. 12 and 13) [cf. Eqs. (4), (5a), and (5b)], which describe the enhancement of density of *individual* electronic states i on the positron site and where r_s corresponds to the effective electron density[5] in the material investigated.

A great deal of caution is necessary when the parameters $\epsilon(p,r_s)$ are compared with experimental EF's of MDAP's, $\tilde{\epsilon}_v(\mathbf{p})$ or $\tilde{\epsilon}_c(\mathbf{p})$. For instance, although the two-particle enhancements $\epsilon(p,r_s)$ are always nondecreasing functions of momentum,[12,13] a decrease of $\tilde{\epsilon}_v(\mathbf{p})$ for d electrons,[22] as well as of $\tilde{\epsilon}_c(\mathbf{p})$,[2,7] with increasing $|\mathbf{p}|$ occurs. Moreover, two-particle EF's $\epsilon(X_i=p,\ r_s)$ are either defined only for $|\mathbf{p}|\le|\mathbf{p}_F|$ (Ref. 13) ($\mathbf{p}_F$ being the Fermi momentum) or have very small values for $|\mathbf{p}|\ge|\mathbf{p}_F|$,[12] whereas the $\tilde{\epsilon}_v(\mathbf{p})$ and $\tilde{\epsilon}_c(\mathbf{p})$ may be calculated for every value of $\mathbf{p}$ [provided $\rho^{\mathrm{IPM}}(\mathbf{p})\neq 0$], and the experimental results on alkali metals show[3,11] that $\tilde{\epsilon}_v(\mathbf{k}+\mathbf{G})$ is of similar (or slightly lower) value as $\tilde{\epsilon}_v(\mathbf{k})$ (here $\mathbf{k}$ lies in the first Brillouin zone and $\mathbf{G}\neq\mathbf{0}$ is a reciprocal lattice vector). Therefore, in the higher-momentum region ($|\mathbf{p}|\ge|\mathbf{p}_F|$), the $\tilde{\epsilon}_v(\mathbf{p})$ cannot be identified with $\epsilon(X_{\mathbf{k}j},r_s)$ at all. The problem of enhancement of valence high-momentum components in real metals was studied recently in Refs. 7 and 14.

Let us discuss the problem within the LDA of Refs. 7, 17, 18, and 22. This approximation corresponds to a replacement of the correlation functions $g(\mathbf{r},i)$ in Eq. (3) by the electron-gas factors $\epsilon[X_i,r_s(\mathbf{r})]$ (e.g., those of Ref. 13). Taking into account Eqs. (1), (1'), (3), (6a), and (6b), one gets

$$\tilde{\epsilon}_x(\mathbf{p})=\frac{\sum_{i_x}\left|\int e^{-i\mathbf{p}\cdot\mathbf{r}}\psi^0_+(\mathbf{r})\psi^0_i(\mathbf{r})\sqrt{\epsilon[X_i,r_s(\mathbf{r})]}d\mathbf{r}\right|^2}{\sum_{i_x}\left|\int e^{-i\mathbf{p}\cdot\mathbf{r}}\psi^0_+(\mathbf{r})\psi^0_i(\mathbf{r})d\mathbf{r}\right|^2} , \tag{7}$$

where x stands for core or valence electronic states.

First, the case of valence electrons in the low-momentum region ($|\mathbf{p}|\le|\mathbf{p}_F|$) will be considered. If the products of positron and electron wave functions, $\psi^0_+(\mathbf{r})\psi^0_i(\mathbf{r})$, are localized in the region of almost constant density, i.e., $r_s(\mathbf{r})\simeq r_s$, the AED approach[2,10,15,16] may be used. This may be often supposed for valence electrons in the interstitial region, but it is generally not satisfied for core and d electrons.

The EF's $\tilde{\epsilon}_x(\mathbf{p})$ [Eqs. (6a) and (6b)] can be identified with the two-particle enhancements $\epsilon[p,r_s(\mathbf{r})]$ only in two cases:

(1) Electron and positron wave functions are single plane waves. This is rather well satisfied in nearly parabolic valence bands, where the high-momentum components of electron wave functions are small and may be, as an approximation, neglected. In this case the electron density is obviously constant, $X_{\mathbf{k}j}=\sqrt{E_{\mathbf{k}j}/E_F}\approx k$, and the EF's $\tilde{\epsilon}_x(\mathbf{p})$ are equal to $\epsilon(X_{\mathbf{p}j}=p,\ r_s)$. Of course, core and d electrons are strongly distorted from single plane waves, and therefore they cannot be considered in this case.

(2) The $\epsilon[X_i,r_s(\mathbf{r})]$ are almost constant, i.e., $\epsilon[X_i,r_s(\mathbf{r})]\simeq\gamma_x$. This condition is, however, hardly fulfilled in practice. It might hold "in average" either, e.g., for narrow d-electron bands or for certain core states where $\epsilon(\bar{X}_i,\bar{r}_s)$ ($\bar{X}_i$ and $\bar{r}_s$ being some mean values) yields some representative average of $\epsilon[X_i,r_s(\mathbf{r})]$, or for very high electron densities, characterized by $r_s\le 0.1$ a.u. (as it is found near nuclei). In this case $\tilde{\epsilon}_x(\mathbf{p})=\gamma_x=\lambda_x/\lambda_x^{\mathrm{IPM}}$ is also constant and equal to $\epsilon(\bar{X}_i,\bar{r}_s)$. However, as was mentioned above, the condition of constant electron density is not fulfilled in ionic cores, and therefore the LDA (Refs. 7 and 17) is apparently more appropriate. Although the energy parameters X_i are constant for core states, the change in the electron-density parameter $r_s(\mathbf{r})$ combines with the effect of the distortion of $\psi^0_i(\mathbf{r})$ from plane waves. This effect is pronounced in the region intermediate between interstitial and nuclei ones, where the product of positron and core electron densities achieves its maximum, and the function $r_s(\mathbf{r})$ neither can be treated as a constant nor are its values small (less than 0.1 a.u.). Exceptions might be the atoms with relatively dense cores, providing nearly constant $\tilde{\epsilon}_c(\mathbf{p})$ (e.g., at the end of each series of metals Na–Al, K–Zn, and Rb–Cd, as was found in Ref. 2).

Therefore, except for the two cases mentioned above, for $|\mathbf{p}|\le|\mathbf{p}_F|$ the momentum dependence of the EF's $\tilde{\epsilon}_v(\mathbf{p})$ [Eqs. (6a) and (6b)] differs from the one of the two-

particle parameters $\epsilon(p,\bar{r}_s)$, and the values of $\bar{\epsilon}_v(\mathbf{p})$ can be obtained based on $\epsilon(p,\bar{r}_s)$ only if the electron and positron wave functions are known [via Eq. (7)]. For the ionic core electrons, there is also no direct connection between $\bar{\epsilon}_c(\mathbf{p})$ and the two-particle EF's $\epsilon[0,r_s(\mathbf{r})]$ employed for the core [cf. Eq. (5b)]. The two-particle EF's do not even depend on momentum at all, in contrast to $\bar{\epsilon}_c(\mathbf{p})$. The connection between both EF's may be obtained again through Eq. (7).

A common feature of the approximations used in Refs. 2, 7, 10, and 15–18 is that they take into account the enhancement of the density of individual electronic states on the positron site, but they neglect the distortion of the positron wave function from its IPM value ψ_+^0 due to positron interaction with the electronic screening cloud $\Delta n(\mathbf{r}_{e^-},\mathbf{r}_{e^+})$. Within the IPM the positron is repelled to the interstitial region by repulsive Coulomb potential $-V_C$, where V_C is the Hartree part of the electron crystal potential. This is properly described by the unperturbed positron wave function ψ_+^0. However, if the positron is screened, it experiences also the attractive electron-positron correlation potential $V_{\rm corr}$ (Ref. 12) due to the change of electron density around a positron, which slightly diminishes the repulsion $-V_C$. To describe this effect, one adds the correlation potential $V_{\rm corr}$ to the Coulomb potential $-V_C$ in the positron Schrödinger equation. The resulting "correlated" positron wave function $\psi_+^{\rm corr}(\mathbf{r})$ is extended slightly more into the center of the atom in comparison with $\psi_+^0(\mathbf{r})$ (here and henceforth the $\psi_+^{\rm corr}$ is calculated from the condition of zero logarithmic derivative at the Wigner-Seitz radius). In Fig. 1 the shapes of $\psi_+^0(\mathbf{r})$ and $\psi_+^{\rm corr}(\mathbf{r})$ in a simple and transition metal, namely, (a) Na and (b) Fe, are compared. The $\psi_+^0(\mathbf{r})$ are denoted by solid lines, and the difference curves $\psi_+^{\rm corr}(\mathbf{r})-\psi_+^0(\mathbf{r})$ are presented by dashed lines. The corresponding pair-correlation functions $g(\mathbf{r},i)$ are then approximated by $\epsilon[0,r_s(\mathbf{r})][\psi_+^{\rm corr}(\mathbf{r})/\psi_+^0(\mathbf{r})]^2$; i.e., the pair wave functions [Eq. (3)] are given by $\psi_i^{e^-e^+}(\mathbf{r},\mathbf{r})=\psi_+^{\rm corr}(\mathbf{r})\psi_i^0(\mathbf{r})\sqrt{\epsilon[0,r_s(\mathbf{r})}$.

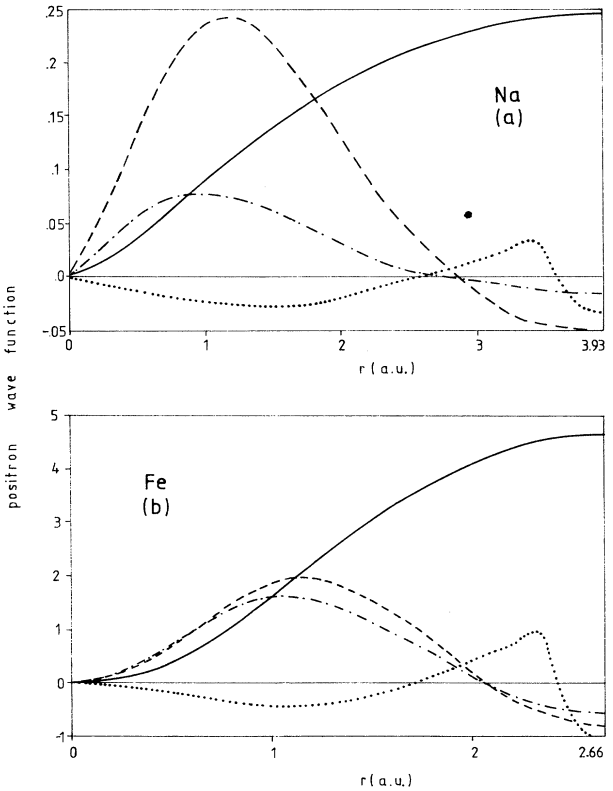

FIG. 1. Positron wave function in (a) Na and (b) Fe. Solid line, $\psi_+^{0,\rm HL}$ calculated using the $V_{\rm xc}^{\rm HL}$ in the electron crystal potential; dashed line, the difference curve $\psi_+^{\rm corr,HL}-\psi_+^{0,\rm HL}$; chained line, $\psi_+^{0,S}-\psi_+^{0,\rm HL}$; dotted line, $\psi_+^{\rm APW,S}-\psi_+^{0,S}$. The difference curves are magnified 20 times in comparison with $\psi_+^{0,\rm HL}$.

The above way of treating the positron wave function in real metals is generally applied to calculations of MDAP's and annihilation rates of positrons trapped at vacancies and metal surfaces,[19,20] where the positron is strongly localized just near the correlation potential. Puska and Nieminen[6] and Jensen[6] employed the $V_{\rm corr}$ also in the calculation of partial and total annihilation rates in simple and transition metals without, however, determining MDAP's and momentum dependence of EF's. Only Chakraborty[5] calculated core MDAP's and EF's in bulk Al using $V_{\rm corr}$ in the positron Schrödinger equation, but within the AED approach.

In the present paper the $V_{\rm corr}$ is also taken into account in the calculation of MDAP's and EF's in the bulk undefected metals, but we use the local approach. The attention is focused mainly on positron annihilation with rare-gas core electrons. The formalism, however, can be applied to calculations of valence and total MDAP's and EF's as well.

III. EFFECT OF SOME PARAMETERS IN THE CALCULATION OF ELECTRON AND POSITRON WAVE FUNCTIONS ON THE RARE-GAS CORE POSITRON-ANNIHILATION CHARACTERISTICS: IPM RESULTS

For the study of the influence of various characteristics of positron and electron wave functions on the rare-gas core annihilation, the IPM seems to be most convenient because in this model [Eqs. (1′) and (2′)] the picture is not deformed by correlation effects, which will be dealt in the next section. The rare-gas core electron wave functions were calculated nonrelativistically as well as relativistically using the code of Herman and Skillman[23] and of Liberman, Cromer, and Waber,[24] respectively, with the Hedin-Lundqvist (HL) or Slater (S) exchange-correlation potentials $V_{\rm xc}^{\rm HL}$ and $V_{\rm xc}^S$, respectively. The corresponding Coulomb positron potentials $-V_C^{\rm HL}$ and $-V_C^S$ were generated by superposition of atomic electron densities following the Mattheiss construction scheme.[25] The IPM positron wave function was obtained either from the condition of zero logarithmic derivative at the Wigner-Seitz radius $r_{\rm WS}$ $[\psi_+^0(r)]$ or as a single augmented plane-wave function at $\mathbf{k}=0$ with only $l=0$ terms included $[\psi_+^{\rm APW}(r)]$. The latter approximation is often used in the calculation of the MDAP. The IPM MDAP's corresponding to the nlj core shell in the relativistic case calculated according to the formula [cf. Eqs. (1′)]

$$\rho^{\mathrm{IPM}}_{c,nlj}(p)=4\pi(2j+1)\left\{\left|\int_0^{r_{\mathrm{WS}}} r^2 A_{nlj}(r)\psi_+(r)j_l(pr)dr\right|^2+\left|\int_0^{r_{\mathrm{WS}}} r^2 B_{nlj}(r)\psi_+(r)j_l(pr)dr\right|^2\right\}, \tag{8}$$

where $A_{nlj}(r)$ and $B_{nlj}(r)$ are the radial components of the relativistic electron wave functions, $j_l(x)$ are spherical Bessel functions of lth order, and ψ_+ stands for ψ_+^0 or ψ_+^{APW} in accordance with the positron wave function used. The IPM MDAP's in the nl core shell in the nonrelativistic case were determined according to formula

$$\rho^{\mathrm{IPM}}_{c,nl}(p)=8\pi(2l+1)\left|\int_0^{r_{\mathrm{WS}}} r^2 R_{nl}(r)\psi_+(r)j_l(pr)dr\right|^2, \tag{9}$$

where $R_{nl}(r)$ is the nonrelativistic radial electron wave function. The core IPM annihilation rate was calculated according to (2′), i.e., from the equation

$$\lambda_c^{\mathrm{IPM}}=\pi r_0^2 c\int dr\, 4\pi r^2|\psi_+(r)|^2 n_c(r), \tag{10}$$

where $\psi_+(r)$ stands either for ψ_+^0 or for ψ_+^{APW} and $n_c(r)$ is the rare-gas core electron density.

Table I summarizes the values of rare-gas core annihilation rates calculated relativistically [Eq. (8)] within the IPM using the exchange-correlation potentials $V_{\mathrm{xc}}^{\mathrm{HL}}$ or V_{xc}^{S} in the atomic structure calculations as well as with different shapes of positron wave functions (ψ_+^0 and ψ_+^{APW}) in ten simple and d metals. Employment of V_{xc}^{S} gives the values of λ_c^{IPM} by 4–6 % lower at the beginning of both series K–Cu and Rb–Ag as well as in Na and Al, almost the same for late d metals (e.g., for Fe) and by 4–7 % higher at the end of both series than obtained using the $V_{\mathrm{xc}}^{\mathrm{HL}}$ (see column 7 in Table I). This is a not so small effect, and one should be aware of it when theoretical and experimental values of annihilation rates are compared. The change of the exchange-correlation potential is also reflected in the height and shape of the corresponding rare-gas core MDAP [cf. the solid and dashed lines in Figs. 2(a) and 2(b)]. It is generally believed that $V_{\mathrm{xc}}^{\mathrm{HL}}$ describes better electron-electron exchange and correlation effects than V_{xc}^{S}, and therefore it will be preferred in our further calculations of MDAP's and EF's.

The influence of the shape of positron wave function is also non-negligible. As it can be seen in Fig. 1 from the difference $\psi_+^{\mathrm{APW},S}-\psi_+^{0,S}$, the ψ_+^0 is extended more into the core region. Thus the overlap of ψ_+^{APW} with core electron wave functions decreases in comparison with using ψ_+^0. As a result, a slight decrease (not bigger than 2–3 %) in λ_c^{IPM} is obtained (see column 8 of Table I). The MDAP's calculated with ψ_+^0 and with ψ_+^{APW}, taking the same exchange-correlation potential, are also not very different [cf. the dashed and dotted lines in Figs. 2(a) and 2(b)].

Of course, the ψ_+^0 calculated from the condition of zero logarithmic derivative at the Wigner-Seitz sphere describes apparently better the positron wave function than a single APW. On the other hand, a positron wave function $\tilde{\psi}_+^{\mathrm{APW}}$ in the form of an APW expansion with several symmetrized terms reflects better the real situation than ψ_+^0. With respect to the spherical symmetry of the rare-gas core, one can hardly expect big differences between the results obtained using ψ_+^0 and $\tilde{\psi}_+^{\mathrm{APW}}$. A single APW is a good first approximation of the positron wave function; however, for a more exact calculation, more terms in the APW expansion should be taken, not only for valence MDAP's,[26] but even for rare-gas core characteristics.

In comparison with the influence of the exchange-correlation potential and of the positron wave function, the importance of relativistic effects is bigger in the heavier elements (column 9 of the Table I). For light simple and early $3d$ metals, the nonrelativistic λ_c^{IPM} differ

TABLE I. Rare-gas core positron-annihilation rates in some simple and d metals calculated relativistically within the independent-particle model. Here a is the lattice constant, $\lambda_c^{\mathrm{IPM}}(\psi_+^0,\mathrm{HL})$, $\lambda_c^{\mathrm{IPM}}(\psi_+^0,S)$, and $\lambda_c^{\mathrm{IPM}}(\psi_+^{\mathrm{APW}},S)$ are the rare-gas core annihilation rates determined with the positron wave function ψ_+^0 or ψ_+^{APW}, using the Hedin-Lundqvist (HL) or Slater (S) exchange correlation in the electron potential (see text). $\eta_{\mathrm{xc}}=\lambda_c^{\mathrm{IPM}}(\psi_+^0,S)/\lambda_c^{\mathrm{IPM}}(\psi_+^0,\mathrm{HL})$ characterizes the influence of various exchange-correlation potentials, $\eta_+=\lambda_c^{\mathrm{IPM}}(\psi_+^{\mathrm{APW}},S)/\lambda_c^{\mathrm{IPM}}(\psi_+^0,S)$ reflects the effect of the shape of the positron wave function, $r=\lambda_c$ (relativistic)/λ_c(nonrelativistic) describes the strength of relativistic effects, and $k=(\Delta\lambda_c/\lambda_c)/(\Delta a/a)$ characterizes the sensitivity of the calculated λ_c to the change in the lattice constant.

1 Metal		2 Configuration	3 a (a.u.)	4 $\lambda_c^{\mathrm{IPM}}(\psi_+^0,\mathrm{HL})$ (10^9 s^{-1})	5 $\lambda_c^{\mathrm{IPM}}(\psi_+^0,S)$ (10^9 s^{-1})	6 $\lambda_c^{\mathrm{IPM}}(\psi_+^{\mathrm{APW}},S)$ (10^9 s^{-1})	7 η_{xc}	8 η_+	9 r	10 k (%)
Na	bcc	$3s^1$	7.984	0.207	0.198	0.193	0.956	0.978	0.998	−4.7
Al	fcc	$3s^2 3p^1$	7.6395	0.263	0.249	0.246	0.947	0.988	0.996	−5.4
K	bcc	$4s^1$	9.874	0.136	0.128	0.125	0.941	0.978	0.996	−5.0
V	bcc	$3d^3 4s^2$	5.723	0.874	0.855	0.842	0.978	0.985	0.994	−5.3
Fe	bcc	$3d^6 4s^2$	5.4065	0.771	0.774	0.761	1.004	0.983	0.986	−5.4
Cu	fcc	$3d^{10} 4s^1$	6.830	0.571	0.610	0.600	1.068	0.984	0.976	−5.0
Rb	bcc	$5s^1$	10.555	0.125	0.118	0.115	0.939	0.973	0.982	−4.9
Nb	bcc	$4d^4 5s^1$	6.237	0.844	0.830	0.821	0.983	0.989	0.977	−5.5
Pd	fcc	$4d^{10}$	7.352	0.654	0.681	0.673	1.042	0.988	0.948	−5.1
Ag	fcc	$4d^{10} 5s^1$	7.689	0.440	0.458	0.452	1.042	0.986	0.942	−5.3

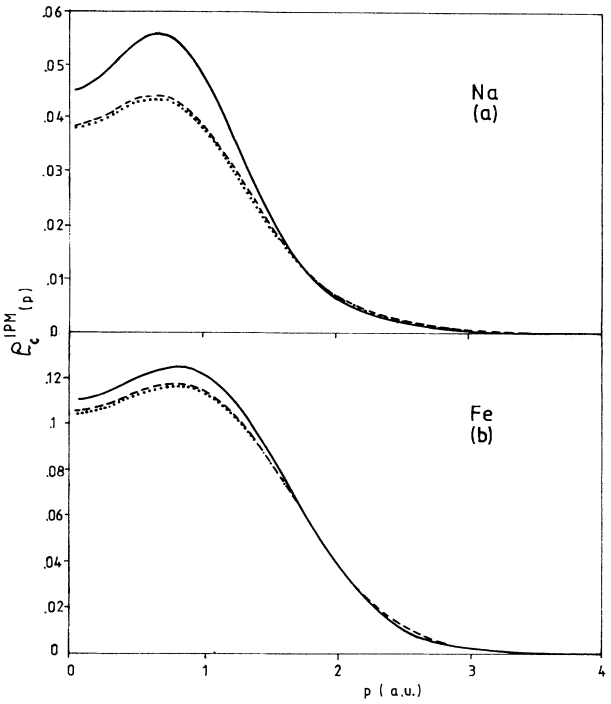

FIG. 2. Rare-gas core momentum densities of annihilation pairs in (a) Na and (b) Fe calculated within IPM. Solid line, $\rho_c^{IPM}(\psi_+^0,HL)$ obtained using ψ_+^0 and V_{xc}^{HL}; dashed line, $\rho_c^{IPM}(\psi_+^0,S)$; dotted line, $\rho_c^{IPM}(\psi_+^{APW},S)$.

only slightly from the relativistic ones.

It turns out that the rare-gas core annihilation rates are very sensitive to the change in the lattice constant a. As may be seen in column 10 of Table I, a change of 1% in the lattice constant a causes a change of about -5% in λ_c^{IPM}. Similar changes are obtained also for λ_c with electron-positron correlation effects included. This effect might be checked experimentally in alkali metals, where the coefficient of thermal expansion is fairly high, and in the two-dimensional ACPAR measurements for the [110] direction, it is possible to isolate the core annihilation in some momentum regions.[3] Let us note here that the change in the itinerant-electron (valence-electron) annihilation rate λ_v^{IPM} within the IPM reflecting the 1% change in the lattice constant is -3% (because of the r_s^{-3} dependence of λ_v^{IPM}), and the corresponding change in λ_v with electron-positron correlations included (which may be roughly estimated according to the Brandt-Reinheimer formula[1]) amounts from -0.5% (Cs) to -2.4% (Pd).

All results collected in Table I are related to atomic configurations given in the column 1. This is not quite correct since the actual band structures of metals do not correspond to free-atom configurations.[27,28] Different choices of electronic configurations, however, yield differences in λ_c^{IPM}, which are comparable with those of columns 7–9 of Table I. For example, λ_c^{IPM} obtained for the configurations $3d^64s^2$ and $3d^74s^1$ in iron using V_{xc}^{HL} and $\psi_+^{0,HL}$ differ by 6.6%. Thus we performed another calculation of the atomic structure, basing on the electronic configurations given in Table V of Ref. 27 or (for Li, Be, Na, Mg, Al, Zn, and Cd) on those of Ref. 28 (furthermore, solid-state configurations). For a better convergence of the computations, a small amount of valence electrons corresponding to the f symmetry has been proportionally distributed into the s, p, and d states (in Li, Be, Na, Mg, and Al, the numbers of electrons of d symmetry were similarly divided into the s and p states). The resulting rare-gas core as well as total annihilation rates are displayed for both types of configurations in Tables II and III, respectively.

To characterize the changes in the IPM values due to changes in the electronic configuration, the quantities

$$r_c^{IPM}=[\lambda_c^{IPM}(\text{atomic})-\lambda_c^{IPM}(\text{solid state})]/\lambda_c^{IPM}(\text{solid state})$$

and

$$r^{IPM}=[\lambda^{IPM}(\text{atomic})-\lambda^{IPM}(\text{solid state})]/\lambda^{IPM}(\text{solid state})$$

(columns 5 and 10 of Table III) were calculated. Here "atomic" and "solid state" mean the atomic and solid-state electronic configurations, respectively, and λ^{IPM} is the IPM total annihilation rate. It may be seen that r_c^{IPM} is relatively high and negative in the case of $3d$ and $4d$ metals where the atomic configuration with two $4s$ or $5s$ electrons was used; this is also the case of Ca (see column 2 of Table II). On the other hand, in Cr, Cu, Nb, Mo, Ag, Pt, and Au, where the configuration with only one outer s electron was employed, the r_c^{IPM} are small and positive. Such atomic configurations are, therefore, apparently somewhat closer to the solid-state electronic configurations, as can be also seen from columns 2–4 of Table III. In Pd, where no outer s electron in the atomic configuration was admitted, the r_c^{IPM} is an absolute value comparable with the r_c^{IPM} of elements where the two outer electrons were taken. For Zn, Cd, and simple metals (except for Ca), the r_c^{IPM} is relatively small.

The r^{IPM} defined for the total IPM annihilation rate has usually the opposite sign than r_c^{IPM} and is also less in absolute value. Thus we have, e.g., about 2% change in the total λ^{IPM} in V and Fe when going from the solid-state to atomic configurations, but about -5% change in the rare-gas core λ_c^{IPM}. The change in the annihilation rate of itinerant (valence) electrons due to the change of electronic configurations goes, therefore, in the opposite direction than the change in the rare-gas core annihilation rate, and as a result, the total annihilation rate does

not change very much when employing the solid-state electronic configuration, especially in the case when the atomic configuration with one outer s electron in $3d$ and $4d$ metals was used. However, the rare-gas core and valence annihilation rates themselves reflect the change in electronic configuration more sensitively, as may be seen by comparison of columns 5 and 10 of Table III (the relative changes in the valence annihilation rate are roughly of the same magnitude, but have the opposite sign). As concerns the rare-gas core and total annihilation rates λ_c^0, λ^0, $\lambda_c^{\rm corr}$, and $\lambda^{\rm corr}$ calculated in the next section with the inclusion of the electron-positron correlation effects, the corresponding ratios r_c^α and r^α (α is 0 or "corr") are very similar to $r_c^{\rm IPM}$ and $r^{\rm IPM}$, respectively. Thus, for a thorough comparison of experimental and theoretical results, solid-state configurations should be taken when calculating the rare-gas core MDAP and annihilation rate.

IV. EFFECT OF ELECTRON-POSITRON CORRELATIONS

In the calculations of core annihilation characteristics presented in this section, the relativistic electron wave functions obtained with $V_{\rm xc}^{\rm HL}$ are used. Both atomic as well as solid-state electronic configurations[27,28] are considered. The positron wave functions satisfy the condition of the zero logarithmic derivative at the Wigner-Seitz sphere. The electron-positron correlations are in-

TABLE II. Positron-annihilation characteristics of 27 simple and d metals calculated using the atomic configuration. Here a and c are the lattice constants, λ_c^0 and $\lambda_c^{\rm corr}$ are the rare-gas core annihilation rates with ψ_+^0 and $\psi_+^{\rm corr}$, respectively, $\gamma_c^0=\lambda_c^0/\lambda_c^{\rm IPM}$ and $\gamma_c^{\rm corr}=\lambda_c^{\rm corr}/\lambda_c^{\rm IPM}$ denote the corresponding core enhancement factors, $\lambda_c^{\rm IPM}$ being the IPM rare-gas core annihilation rate, and λ^0 and $\lambda^{\rm corr}$ are the total annihilation rates calculated with ψ_+^0 and $\psi_+^{\rm corr}$, respectively. Further, column 11 shows, for the sake of comparison, the total annihilation rates of Jensen (Ref. 6). In columns 12 and 13 the core fractions of the total annihilation rate related to the experimental values (given in Table III) are displayed. The last line of the table represents the rms deviations of the total annihilation rates in a given column from the experimental values (except for Ca, Sc, Mn, and Co). All quantities are calculated relativistically using the Hedin-Lundqvist exchange correlation potential.

1 Metal		2 Configuration	3 a (a.u.)	4 c (a.u.)	5 λ_c^0 (10^9 s^{-1})	6 γ_c^0	7 $\lambda_c^{\rm corr}$ (10^9 s^{-1})	8 $\gamma_c^{\rm corr}$	9 λ^0 (10^9 s^{-1})	10 $\lambda^{\rm corr}$ (10^9 s^{-1})	11 λ of Jensen (10^9 s^{-1})	12 $\lambda_c^0/\lambda_{\rm expt}$ (%)	13 $\lambda_c^{\rm corr}/\lambda_{\rm expt}$ (%)
Li	bcc	$2s^1$	6.582		0.408	2.68	0.450	2.96	3.166	3.302	3.390	11.9	13.1
Be	hcp	$2s^2$	4.329	6.783	0.563	1.94	0.593	2.04	6.924	6.954	7.463	8.0	8.4
Na	bcc	$3s^1$	7.984		0.606	2.93	0.702	3.40	2.853	2.935	3.155	20.5	23.7
Mg	hcp	$3s^2$	6.026	9.781	0.589	2.32	0.658	2.59	4.066	4.132	4.386	13.3	14.8
Al	fcc	$3s^23p^1$	7.6395		0.536	2.04	0.585	2.22	5.642	5.697	6.135	8.7	9.5
K	bcc	$4s^1$	9.874		0.605	4.45	0.688	5.07	2.486	2.548	2.755	24.0	27.3
Ca	fcc	$4s^2$	10.548		0.634	3.26	0.704	3.62	3.233	3.292			
Sc	hcp	$3d^14s^2$	6.201	10.125	1.135	2.66	1.230	2.88	4.699	4.794		26.1	28.3
Ti	hcp	$3d^24s^2$	5.522	9.019	1.563	2.34	1.673	2.51	6.300	6.425	7.092	23.0	24.6
V	bcc	$3d^34s^2$	5.723		1.879	2.15	1.997	2.29	7.874	8.024	8.929	24.4	26.0
Cr	bcc	$3d^54s^1$	5.451		2.108	2.04	2.245	2.17	8.864	9.069	10.101	25.3	27.0
Mn	fcc	$3d^54s^2$	6.906		1.615	1.97	1.726	2.11	8.892	9.073			
Fe	bcc	$3d^64s^2$	5.4065		1.469	1.91	1.577	2.05	9.214	9.409	10.204	15.6	16.7
Co	hcp	$3d^74s^2$	4.742	7.746	1.365	1.85	1.470	1.99	9.588	9.799		16.2	17.4
Ni	fcc	$3d^84s^2$	6.658		1.226	1.80	1.326	1.94	9.719	9.944	10.638	13.5	14.6
Cu	fcc	$3d^{10}4s^1$	6.830		1.009	1.77	1.114	1.95	8.639	8.917	9.709	11.1	12.3
Zn	hcp	$3d^{10}4s^2$	5.026	9.188	0.537	1.75	0.607	1.98	6.986	7.202	7.692	8.0	9.0
Rb	bcc	$5s^1$	10.555		0.643	5.13	0.724	5.77	2.406	2.464	2.688	26.1	29.4
Zr	hcp	$4d^25s^2$	6.056	9.890	1.513	2.56	1.611	2.73	5.804	5.909	6.536	25.0	26.6
Nb	bcc	$4d^45s^1$	6.237		1.963	2.33	2.078	2.46	7.349	7.496	8.403	23.4	24.7
Mo	bcc	$4d^55s^1$	5.935		2.089	2.18	2.205	2.30	8.603	8.768	9.709	21.5	22.7
Pd	fcc	$4d^{10}$	7.352		1.271	1.95	1.381	2.11	8.795	9.069	9.901	12.2	13.2
Ag	fcc	$4d^{10}5s^1$	7.689		0.845	1.92	0.935	2.13	7.618	7.878	8.403	11.1	12.3
Cd	hcp	$4d^{10}5s^2$	5.609	10.443	0.456	1.91	0.519	2.17	6.150	6.367	6.757	8.0	9.1
Cs	bcc	$6s^1$	11.487		0.668	6.10	0.742	6.78	2.308	2.358	2.611	27.9	31.1
Pt	fcc	$5d^96s^1$	7.413		1.273	1.89	1.373	2.04	9.656	9.884	10.870	12.6	13.6
Au	fcc	$5d^{10}6s^1$	7.682		0.912	1.88	1.002	2.06	8.546	8.792	9.524	10.7	11.7
$\langle\delta^2\rangle$									0.55	0.52	0.76		

cluded both into electron and positron wave functions. The rare-gas core states $\psi_{i_c}^0(\mathbf{r})$ are enhanced by a factor $\sqrt{\epsilon[0,r_s(\mathbf{r})}$ (cf. Ref. 7), while the valence states $\psi_{kj}^0(\mathbf{r})$ are enhanced by a square root of the two-particle jellium-model EF's,[12,13] averaged over momenta $\mathbf{k}$:

$$\langle \epsilon[k,r_s(\mathbf{r})]\rangle_{\mathbf{k}} = 1+\Delta n(\mathbf{r},\mathbf{r})/n(\mathbf{r}) = \Gamma[n(\mathbf{r})]/\Gamma^{\mathrm{IPM}}[n(\mathbf{r})] .$$

Here $\Gamma[n]$ denotes the annihilation rate, obtained within the model of jellium for the corresponding electron density n in the parametrized form[12]

$$\Gamma[n]=\pi r_0^2 cn(1+1.23r_s+0.8295r_s^{3/2} -1.26r_s^2+0.3286r_s^{5/2}+r_s^3/6) .$$

$\Gamma^{\mathrm{IPM}}[n]=\pi r_0^2 cn$ is the well-known IPM annihilation rate, and $\Delta n(\mathbf{r},\mathbf{r})$ is the density of electronic screening charge on the positron.[12,13] Electron-positron correlations were also included to the positron wave function, as described in Sec. II, provided $\psi_+^{\mathrm{corr}}(\mathbf{r})$. The jellium-model correlation potential $V_{\mathrm{corr}}(\mathbf{r})$ in a parametrized form[12] (cf. also Refs. 5 and 6) was employed in a local way.

To study the effect of including electron-positron correlations into the positron wave function, calculations of MDAP's, annihilation rates, and momentum-dependent EF's were performed by employing also $\psi_+^0(\mathbf{r})$. The corresponding core MDAP's in the nl core shell, $\rho_{c,nl}^0(\mathbf{p})$ and $\rho_{c,nl}^{\mathrm{corr}}(\mathbf{p})$, were calculated according to formulas

TABLE III. Positron-annihilation characteristics of 27 simple and d metals calculated using the solid-state configurations (Refs. 27 and 28). Columns 2–4 give the solid-state configuration used; the symbols λ and γ have the same meaning as in the Table II. Further, $r_c^{\mathrm{IPM}}=[\lambda_c^{\mathrm{IPM}}(\mathrm{atomic})-\lambda_c^{\mathrm{IPM}}(\mathrm{solid\ state})]/\lambda_c^{\mathrm{IPM}}(\mathrm{solid\ state})$ and $r^{\mathrm{IPM}}=[\lambda^{\mathrm{IPM}}(\mathrm{atomic})-\lambda^{\mathrm{IPM}}(\mathrm{solid\ state})]/\lambda^{\mathrm{IPM}}(\mathrm{solid\ state})$ characterize the relative change of core and total IPM positron-annihilation rate due to change from the solid-state to the atomic configuration; relative changes of $\lambda_c^0,\lambda_c^{\mathrm{corr}}$ and $\lambda^0,\lambda^{\mathrm{corr}}$ due to change of the electronic configuration are very similar to r_c^{IPM} and r^{IPM}, respectively. $\langle\delta^2\rangle$ is defined in the same way as in the Table II. All quantities are calculated relativistically using the Hedin-Lundqvist exchange-correlation potential. The experimental values were taken from Ref. 30 except Sc and Co, which were obtained from Ref. 31.

1		2	3	4	5	6	7	8	9	10	11	12	13	14	15
		Configuration			r_c^{IPM}	λ_c^0		$\lambda_c^{\mathrm{corr}}$		r^{IPM}	λ^0	λ^{corr}	λ_{expt}	$\lambda_c^0/\lambda_{\mathrm{expt}}$	$\lambda_c^{\mathrm{corr}}/\lambda_{\mathrm{expt}}$
Metal		s	p	d	(%)	(10^9 s^{-1})	γ_c^0	(10^9 s^{-1})	γ_c^{corr}	(%)	(10^9 s^{-1})	(10^9 s^{-1})	(10^9 s^{-1})	(%)	(%)
Li	bcc	0.53	0.47		0.1	0.405	2.66	0.447	2.94	0.06	3.165	3.201	3.44	11.8	13.0
Be	hcp	0.47	1.53		−0.7	0.560	1.93	0.592	2.04	0.6	6.886	6.919	7.04	8.0	8.4
Na	bcc	0.75	0.25		0.4	0.604	2.92	0.699	3.38	0.02	2.852	2.933	2.96	20.4	23.6
Mg	hcp	0.81	1.19		1.6	0.584	2.30	0.648	2.55	−0.6	4.077	4.137	4.44	13.2	14.6
Al	fcc	1.59	1.41		0.8	0.533	2.03	0.580	2.21	−0.4	5.656	5.708	6.13	8.7	9.5
K	bcc	0.666	0.334		0.4	0.602	4.43	0.685	5.04	0.08	2.485	2.546	2.52	23.9	27.2
Ca	fcc	0.855	0.661	0.482	−6.9	0.686	3.53	0.765	3.94	3.1	3.177	3.246			
Sc	hcp	0.764	0.680	1.556	−6.1	1.216	2.85	1.325	3.10	2.9	4.593	4.707	4.35	28.0	30.5
Ti	hcp	0.694	0.732	2.574	−5.3	1.659	2.48	1.783	2.67	2.5	6.158	6.306	6.80	24.4	26.2
V	bcc	0.646	0.702	3.652	−5.1	1.988	2.28	2.121	2.43	2.3	7.692	7.871	7.69	25.9	27.6
Cr	bcc	0.633	0.787	4.580	0.9	2.086	2.02	2.220	2.15	−0.2	8.884	9.084	8.33	25.0	26.7
Mn	fcc	0.653	0.794	5.553	−4.8	1.700	2.08	1.824	2.23	2.1	8.701	8.909			
Fe	bcc	0.640	0.759	6.601	−5.2	1.554	2.02	1.674	2.17	2.2	9.004	9.230	9.43	16.5	17.8
Co	hcp	0.650	0.747	7.603	−5.3	1.445	1.95	1.562	2.11	2.2	9.369	9.613	8.45	17.1	18.5
Ni	fcc	0.656	0.727	8.617	−5.6	1.301	1.91	1.414	2.07	2.2	9.493	9.753	9.09	14.3	15.6
Cu	fcc	0.703	0.737	9.560	2.0	0.989	1.73	1.089	1.91	−0.6	8.696	8.956	9.09	10.9	12.0
Zn	hcp	1.440	0.560	10.00	−1.1	0.543	1.77	0.614	2.00	0.4	6.957	7.178	6.76	8.0	9.1
Rb	bcc	0.699	0.301		0.3	0.640	5.10	0.720	5.74	0.1	2.405	2.462	2.46	26.0	29.3
Zr	hcp	0.732	0.674	2.594	−3.4	1.572	2.66	1.680	2.84	2.0	5.711	5.833	6.06	25.9	27.7
Nb	bcc	0.673	0.664	3.663	0.4	1.953	2.31	2.067	2.45	0.01	7.348	7.493	8.40	23.3	24.6
Mo	bcc	0.666	0.815	4.519	0.8	2.070	2.16	2.183	2.28	−0.1	8.614	8.775	9.71	21.3	22.5
Pd	fcc	0.624	0.662	8.714	4.1	1.217	1.86	1.317	2.01	−1.3	8.923	9.163	10.42	11.7	12.6
Ag	fcc	0.693	0.672	9.635	0.7	0.837	1.91	0.926	2.11	−0.1	7.629	7.883	7.63	11.0	12.1
Cd	hcp	1.18	0.82	10.00	−1.4	0.462	1.93	0.526	2.20	0.6	6.116	6.335	5.71	8.1	9.2
Cs	bcc	0.728	0.272		0.1	0.660	6.03	0.736	6.72	0.3	2.308	2.359	2.39	27.6	30.8
Pt	fcc	0.773	0.855	8.372	0.5	1.264	1.88	1.364	2.03	−0.004	9.658	9.883	10.10	12.5	13.5
Au	fcc	0.811	0.792	9.397	0.8	0.903	1.86	0.991	2.04	−0.1	8.560	8.800	8.55	10.6	11.6
$\langle\delta^2\rangle$											0.54	0.50			

$$\rho^{\alpha}_{c,nl}(p)=\sum_j 4\pi(2j+1)\left\{\left|\int_0^{r_{\rm WS}} r^2 A_{nlj}(r)\sqrt{\epsilon[0,r_s(r)]}\psi^{\alpha}_{+}(r)j_l(pr)dr\right|^2+\right.$$
$$\left.+\left|\int_0^{r_{\rm WS}} r^2 B_{nlj}(r)\sqrt{\epsilon[0,r_s(r)]}\psi^{\alpha}_{+}(r)j_l(pr)dr\right|^2\right\}, \tag{11}$$

where α stands either for 0 or for "corr," according to the positron wave function used.

The rare-gas core and total annihilation rates were obtained according to [cf. Eqs. (2), (3), and (5a)]

$$\lambda^{\alpha}_c=\sum_{nl}\lambda_{nl}=\sum_{nl}\pi r_0^2 c\sum_j 4\pi\int r^2|\psi^{\alpha}_{+}(r)|^2[A^2_{nlj}(r)+B^2_{nlj}(r)]\epsilon[0,r_s(r)]dr$$
$$=\pi r_0^2 c\,4\pi\int r^2|\psi^{\alpha}_{+}(r)|^2 n_c(r)\epsilon[0,r_s(r)]dr\ , \tag{12a}$$

and ($n_v=n-n_c$ is the valence-electron density)

$$\lambda^{\alpha}=\lambda^{\alpha}_c+\pi r_0^2 c\int d\mathbf{r}|\psi^{\alpha}_{+}(\mathbf{r})|^2 n_v(\mathbf{r})\Gamma[n(\mathbf{r})]/\Gamma^{\rm IPM}[n(\mathbf{r})]$$
$$=\lambda^{\alpha}_c+4\pi\int dr\, r^2|\psi^{\alpha}_{+}(r)|^2\Gamma[n(r)]n_v(r)/n(r)\ , \tag{12b}$$

respectively. This approach differs from that of Jensen[6] who either enhanced core and valence states by the same enhancement factor (i.e., by $\Gamma[n(r)]/\Gamma^{\rm IPM}[n(r)]$) or neglected the enhancement of core electron density on the positron at all [i.e., in Eq. (12b) he used the $\lambda_c^{\rm corr,IPM}$, given by Eq. (10) with $\psi_+^{\rm corr}$, instead of λ_c^{α} of Eq. (12a); the quantity $\lambda_c^{\rm corr,IPM}$ is discussed below]. In Table II the values of the total annihilation rates λ^0 and $\lambda^{\rm corr}$ obtained for atomic configurations according to formulas (12a) and (12b) (columns 9 and 10) are compared with those following from the use of the two-particle EF's $\Gamma[n(r)]/\Gamma^{\rm IPM}[n(r)]$ applied in Ref. 6 (column 11). The values of $\lambda^{\rm corr}$ from column 10 are lower than those presented in column 11, as the present EF's applied to core electrons, $\epsilon[0,r_s(r)]$, are less than $\Gamma[n(r)]/\Gamma^{\rm IPM}[n(r)]=\epsilon[\bar{k},r_s(r)]$ used in Ref. 6 ($\bar{k}\geq 0$). The experimental data are given in column 13 of Table III. It can be seen that for the majority of metals the values of $\lambda^{\rm corr}$ (column 10 of Table II) are intermediate between experimental data and those of Ref. 6.

The momentum-dependent rare-gas core EF's $\tilde{\epsilon}^{\alpha}_c(\mathbf{p})=\rho^{\alpha}_c(\mathbf{p})/\rho^{\rm IPM}_c(\mathbf{p})$ and their momentum averages $\gamma^{\alpha}_c=\lambda^{\alpha}_c/\lambda^{\rm IPM}_c$ were calculated for both positron models as well. It should be noted here that $\gamma_c^{\rm corr}$ defined in this work differ from those presented by Jensen.[6] Namely, although the theoretical backgrounds to obtain $\lambda_c^{\rm corr}$ were similar in both calculations (except the fact that the present two-particle local enhancement factors were less than the ones used in Ref. 6, as it has been pointed out), we calculated $\lambda_c^{\rm IPM}$ within the true IPM, while Jensen employed $\psi_+^{\rm corr}$ in his "IPM" calculations. The latter approach is internally inconsistent because the existence of an electronic screening cloud $\Delta n(\mathbf{r}_{e^-},\mathbf{r}_{e^+})$ is assumed through $V_{\rm corr}$ and simultaneously neglected by the IPM assumption $\epsilon[p,r_s(R)]\equiv 1$.

The results for the rare-gas core and total annihilation rates are presented in Tables II (for the atomic configuration) and III (for the solid-state configuration). The influence of electronic configuration on λ^{α} and λ^{α}_c is similar to the IPM case (cf. columns 5 and 10 of Table III), and it was discussed in Sec. III.

The inclusion of electron-positron correlations to the positron wave function causes an increase of partial and total annihilation rates. In spite of a rather slight (from 0.4% in Be up to 3.5% in Cd) increase of the total annihilation rate $\lambda^{\rm corr}$ with respect to λ^0, providing a decrease of the positron lifetime τ of few picoseconds only (cf. columns 9 and 10 of Table II and columns 11 and 12 of Table III), the differences in corresponding core annihilation rates are significant (cf. columns 5 and 7 of Table II and columns 6 and 8 of Table III). The influence of $V_{\rm corr}$ in the rare-gas core annihilation rate [characterized by $(\lambda_c^{\rm corr}-\lambda_c^0)/\lambda_c^0$] is more pronounced in simple and noble metals as well as in Zn and Cd (9–16 %) than in $3d$ and $4d$ metals (6–9 %). This effect exceeds the influence of any electron and positron model parameters on the IPM core annihilation rates considered in Sec. III (cf. columns 7–10 of Table I as well as the columns 5 and 10 of Table III), being comparable in magnitude only with the changes in $\lambda_c^{\rm IPM}$ occurring when $V_{\rm xc}^{\rm HL}$ is replaced by $V_{\rm xc}^{S}$. The differences are pronounced for deep-lying core states, being as large as 53–54 % for $2s$ and $2p$ electrons in potassium or about 45% for $1s$ electrons in Na (cf. Table IV where the average enhancement factors in the nl core shell, $\gamma^{\alpha}_{nl}=\lambda^{\alpha}_{c,nl}/\lambda^{\rm IPM}_{c,nl}$, as well as the relative differences $\eta_{nl}=(\gamma^{\rm corr}_{c,nl}-\gamma^0_{c,nl})/\gamma^0_{c,nl}$ in Na, Al, K, Fe, and Cu are given). It is worthwhile to note here that in Na, Al, and Fe, the ratios $\lambda^{\rm corr}_{c,nl}/\lambda^0_{c,nl}$ decrease with increasing shell numbers n and l, while in K and Cu they achieve their maxima for $2s$ states.

Contrary to the effect of the electronic configuration, the annihilation rate from itinerant (valence) electrons λ_v changes in the same direction as the rare-gas core annihilation rate when $V_{\rm corr}$ in the positron wave function is switched on. However, the relative changes in λ_v, which is substantially bigger than λ_c, are much lower. That is why the total annihilation rate is not very sensitive to the inclusion of $V_{\rm corr}$.

In Fig. 3 the momentum dependence of $\rho^{\rm corr}(p)$ [Eq. (11)], which is at the center of interest of the present

TABLE IV. Rare-gas core annihilation rates for individual core shells in some simple and d metals. Here $\lambda_{c,nl}^{\rm corr}$ and $\lambda_{c,nl}^{0}$ are calculated relativistically with $\psi_{+}^{\rm corr}$ and ψ_{+}^{0}, respectively, using the solid-state electronic configurations and the Hedin-Lundqvist exchange-correlation potential. Further, $\gamma_{c,nl}^{\rm corr}=\lambda_{c,nl}^{\rm corr}/\lambda_{c,nl}^{\rm IPM}$, $\gamma_{c,nl}^{0}=\lambda_{c,nl}^{0}/\lambda_{c,nl}^{\rm IPM}$, and $\eta_{nl}=(\gamma_{c,nl}^{\rm corr}-\gamma_{c,nl}^{0})/\gamma_{c,nl}^{0}$ characterize the change in the shell enhancement factor (and in the shell annihilation rate) due to inclusion of $V_{\rm corr}$ in the positron wave function.

	Na	Al	K	Fe	Cu	nl
$\lambda_{c,nl}^{\rm corr}$	0.158×10^{-2}	0.135×10^{-2}	0.5×10^{-5}	0.13×10^{-4}	0.6×10^{-5}	
$\gamma_{c,nl}^{0}$	1.257	1.216	1.2	1.1	1.1	$1s$
$\gamma_{c,nl}^{\rm corr}$	1.814	1.479	1.15	1.12	1.2	
η_{nl}	44.3%	21.6%	30%	26%	9%	
$\lambda_{c,nl}^{\rm corr}$	0.135	0.137	0.945×10^{-3}	0.398×10^{-2}	0.246×10^{-2}	
$\gamma_{c,nl}^{0}$	2.408	1.935	1.488	1.293	1.245	$2s$
$\gamma_{c,nl}^{\rm corr}$	2.893	2.125	2.288	1.548	1.520	
η_{nl}	20.1%	9.8%	53.8%	19.7%	22.1%	
$\lambda_{c,nl}^{\rm corr}$	0.562	0.442	0.245×10^{-2}	0.928×10^{-2}	0.547×10^{-2}	
$\gamma_{c,nl}^{0}$	3.091	2.082	1.497	1.298	1.253	$2p$
$\gamma_{c,nl}^{\rm corr}$	3.511	2.261	2.292	1.552	1.526	
η_{nl}	13.6%	8.6%	53.1%	19.6%	21.8%	
$\lambda_{c,nl}^{\rm corr}$			0.100	0.334	0.218	
$\gamma_{c,nl}^{0}$			3.372	1.801	1.673	$3s$
$\gamma_{c,nl}^{\rm corr}$			4.036	1.963	1.864	
η_{nl}			19.7%	9.0%	11.4%	
$\lambda_{c,\rm nl}^{\rm corr}$			0.581	1.327	0.863	
$\gamma_{c,nl}^{0}$			4.708	1.942	1.797	$3p$
$\gamma_{c,nl}^{\rm corr}$			5.303	2.083	1.972	
η_{nl}			12.6%	7.3%	9.7%	

work, as well as of $\bar{\epsilon}_c^{0}(p)$ and $\bar{\epsilon}_c^{\rm corr}(p)$ in ten metals quoted in Table I are presented by solid, dashed, and dotted lines, respectively. They are calculated for the solid-state configurations given in Table III. It should be pointed out that the EF's $\bar{\epsilon}_c^{0}(p)$ (or their averages γ_c^{0}) reflect the enhancement of core electron density on the positron site (uncontaminated by the change in positron wave function), whereas the differences between $\bar{\epsilon}_c^{\rm corr}(p)$ and $\bar{\epsilon}_c^{0}(p)$ (or between $\gamma_c^{\rm corr}$ and γ_c^{0}) correspond to the effect of including electron-positron correlations into the positron wave function. Employment of $\psi_{+}^{\rm corr}$ instead of ψ_{+}^{0} causes an increase in rare-gas core EF's $\bar{\epsilon}_c^{\rm corr}(p)$ [and therefore in the MDAP's $\rho_c^{\rm corr}(p)$] in comparison with $\bar{\epsilon}_c^{0}(p)$ [$\rho_c^{0}(p)$] in all the metals [the magnitude of this increase is well described by the ratios $(\lambda_c^{\rm corr}-\lambda_c^{0})/\lambda_c^{0}$ discussed above]. The enhancement of the density of individual electronic states at the positron position, taken into account through the EF's $\epsilon[0,r_s(r)]$, has without doubt the most crucial effect on resulting core MDAP's: The EF's $\bar{\epsilon}_c^{\alpha}(p)$ achieve values as large as 8 in Rb. In the low-momentum region (until 15–20 mrad), both $\bar{\epsilon}_c^{\rm corr}(p)$ and $\bar{\epsilon}_c^{0}(p)$ are decreasing functions of momentum (except a small increase for momenta up to 0.5–1 a.u.), in spite of the two-particle EF's $\epsilon[0,r_s(r)]$, which are constant with respect to the first variable. The decrease of $\bar{\epsilon}_c(p)$ is weaker in Cu, Al, and Fe, and more pronounced in Na, Rb, and Nb, in agreement with the earlier predictions of Refs. 2 and 3. The oscillations in $\bar{\epsilon}_c^{\alpha}$ occurring at higher momenta correspond to relatively small values of $\rho_c^{\alpha}(p)$, and therefore they are not important for the present analysis.

It may be seen from Table II, columns 6 and 8, and Table III, columns 7 and 9, that the values of the average rare-gas core enhancement factors γ_c^{0} and $\gamma_c^{\rm corr}$ are not, except for Li and 4d metals, very different from those obtained in Ref. 2 for the low-momentum ($\leq$15–20 mrad) region. Also the relative rare-gas core fractions $\lambda_c/\lambda_{\rm expt}$ of Ref. 2, recently identified with the fraction of a wide Gaussian in long-slit ACPAR spectra of some metals,[4] agree, again except for Li and 4d metals, quite well with the present values (columns 12 and 13 of Table II, columns 14 and 15 of Table III). The disagreement for Li is apparently due to an inappropriate value of the Gaussian fraction used.[2] Further, Fig. 3 shows that the values of $\bar{\epsilon}_c^{0}$ and $\bar{\epsilon}_c^{\rm corr}$ in the high-momentum region are also not very far from the corresponding high-momentum averages calculated in Ref. 2 [this may be especially well seen in Figs. 3(c), 3(d), and 3(g), where the central peak of $\bar{\epsilon}_c^{0}$ and $\bar{\epsilon}_c^{\rm corr}$ is relatively narrow; cf. also Fig. 2 of the first item in Ref. 7]. Thus, in some sense, the results obtained here constitute some theoretical confirmation of the semiempirical approach of Ref. 2.

Further, it should be noted here that it is possible to determine "effective" average electron density[2,5] in the nl

core shell (with respect to ψ_+^α) based on the values of γ_{nl}^α from the equation $\gamma_{nl}^\alpha=\epsilon(0,\bar{r}_{s,nl})$. The total rare-gas core AED can be obtained in a similar way, by using $\gamma_c^\alpha=\epsilon(0,\bar{r}_{s,c})$, as well as for valence states where one requires $\gamma_v=\Gamma[\bar{n}_v]/\Gamma^{\rm IPM}[\bar{n}_v]$. For example, as it may be determined on the basis of values of $\epsilon(0,r_s)$ from the second item of Ref. 13, in Cu the density of screening cloud "seen" by the positron wave function $\psi_+^{\rm corr}$ is the same as in electron gas of the density parameter $\bar{r}_s=0.27$, 0.64, 0.64, 0.97, and 1.07 for $1s$, $2s$, $2p$, $3s$, and $3p$ states, respectively, and $\bar{r}_{s,c}=1.04$. For the positron wave function ψ_+^0, the corresponding AED parameters are equal to 0.14, 0.33, 0.33, 0.80, and 0.97, respectively, and $\bar{r}_{s,c}=0.88$. The comparison of the $\bar{r}_{s,c}$ values with the r_s obtained for the individual shells also confirms that the highest shells are decisive in the positron annihilation with the rare-gas core electrons.

Finally, let us discuss a comparison of the theoretical total annihilation rates calculated with use of different approaches with the experimental results. We have determined the root-mean-square (rms) deviations $\langle\delta^2\rangle$ of the results in columns 9–11 of Table II and columns 11 and 12 of Table III from the experimental values of the total annihilation rates (column 13 of Table III). The rms deviations were calculated without Sc and Co, which were not treated by Jensen[6] either, and without Ca and Mn, where, according to our knowledge, no experimental lifetimes were published. The corresponding values of

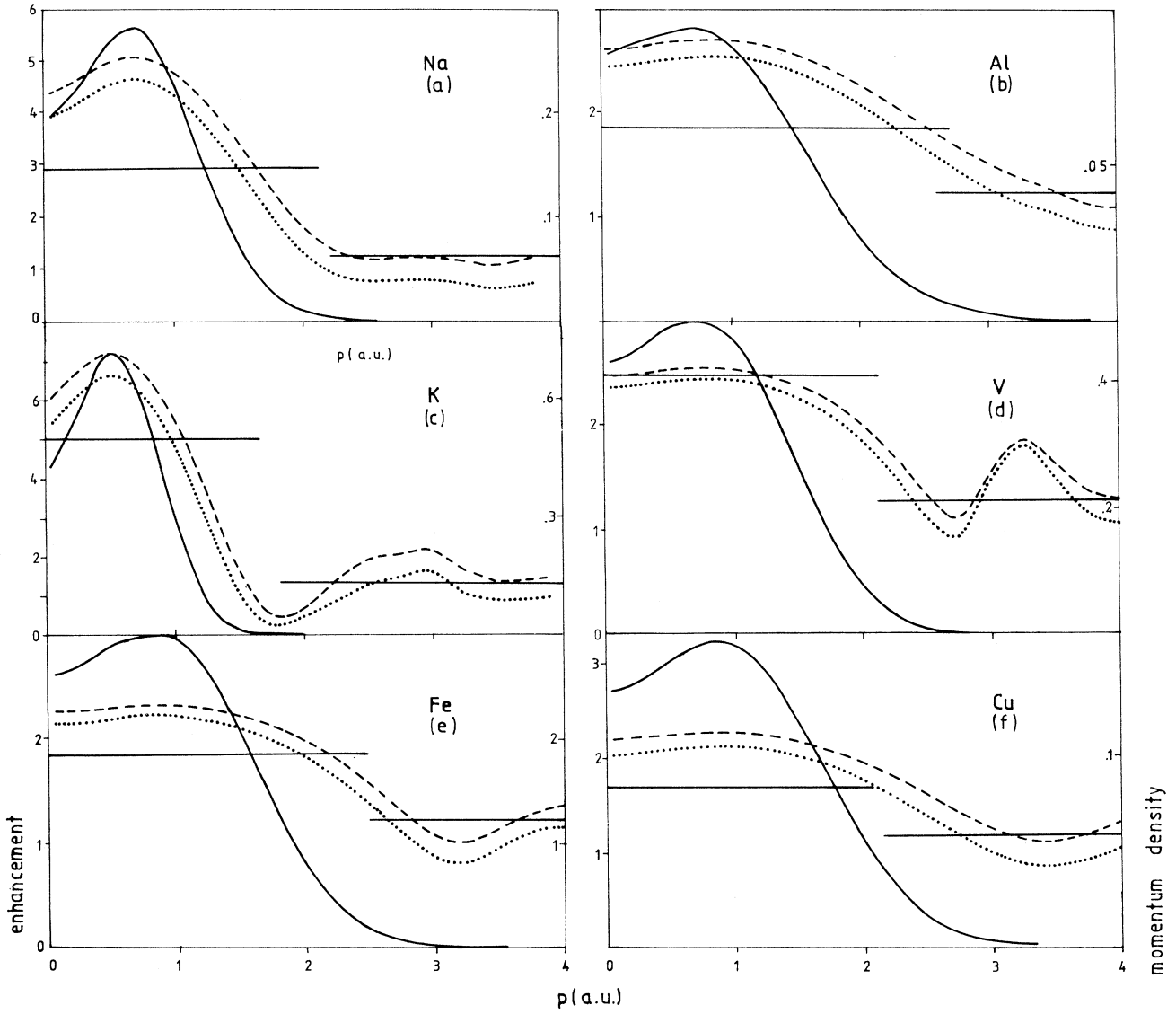

FIG. 3. Rare-gas core momentum densities of annihilation pairs $\rho_c^{\rm corr}(p)$ calculated from $\psi_+^{\rm corr}$ and using $V_{\rm xc}^{\rm HL}$ (solid line) and the corresponding enhancement factors $\bar{\epsilon}_c^{\rm corr}(p)=\rho_c^{\rm corr}(p)/\rho_c^{\rm IPM}(p)$ (dashed line) as well as $\bar{\epsilon}_c^{0}(p)=\rho_c^{0}(p)/\rho_c^{\rm IPM}(p)$ (dotted line). Here ρ_c^0 and $\rho_c^{\rm IPM}$ are calculated from $\psi_+^{0,\rm HL}$, $\rho_c^{\rm IPM}$ being the IPM value. The horizontal lines correspond to the average values of $\bar{\epsilon}_c^{0}$ in the low- and high-momentum regions obtained in Ref. 2.

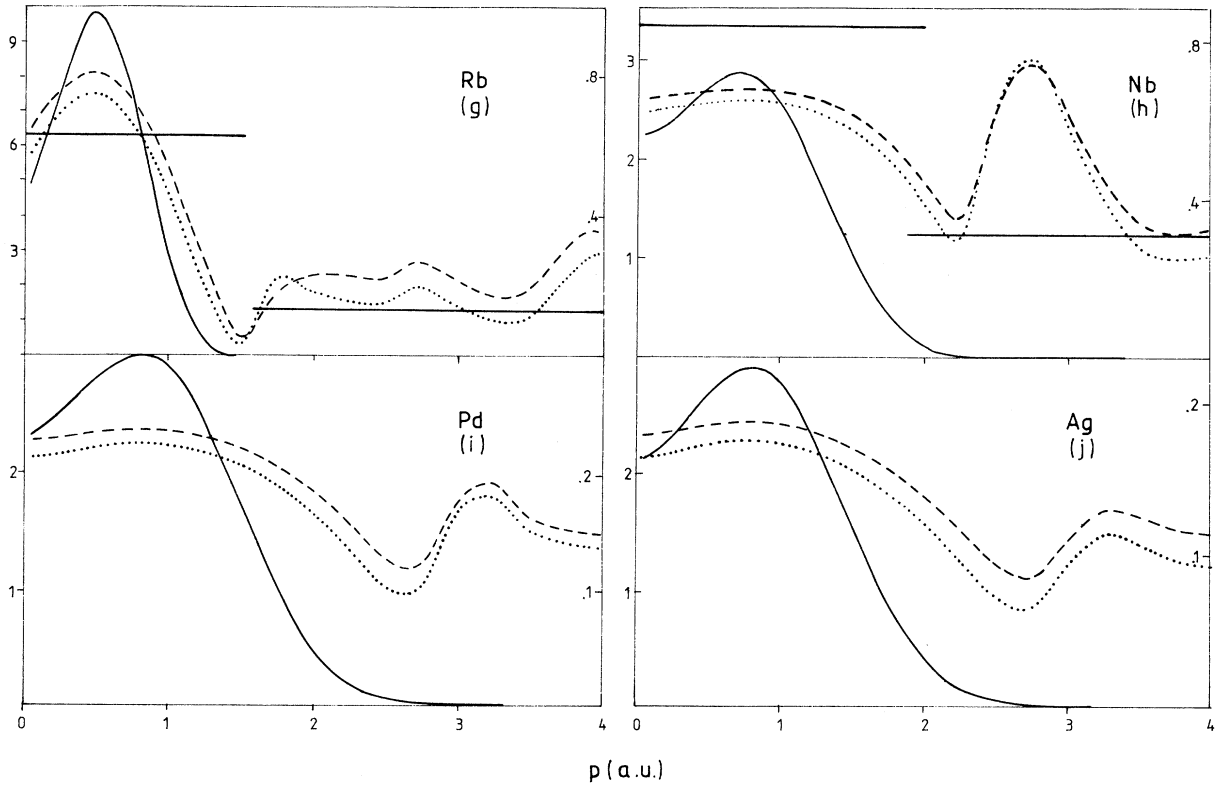

FIG. 3. (*Continued*).

$\langle \delta^2 \rangle$ were equal to 0.55, 0.52, and 0.76 (columns 9–11 of Table II), 0.54 and 0.50 (columns 11 and 12 of Table III), respectively, all quantities in units of 10^9 s^{-1} (see also the last lines in Tables II and III). It may be seen that on average the present approach with V_{corr} in the positron wave function included gives us the best agreement with experiment, the solid-state electronic configurations being slightly favorized. Our values of λ^0 give somewhat bigger rms deviation from experimental data, and the highest $\langle \delta^2 \rangle$ is obtained for column 11 of the Table II, which contains Jensen's[6] results. Thus Eqs. (12a) and (12b) with V_{corr} in the positron wave function included and with the solid-state electronic configuration employed seem to yield a most realistic description of the total annihilation rates and, presumably, also of the rare-gas core positron-annihilation characteristics.

V. CONCLUSIONS

The momentum densities of positron-annihilation pairs, positron-annihilation rates, and electron-positron enhancement factors for rare-gas core electrons in 27 simple and *d* metals were determined using various parameters in the calculation of electron and positron wave functions. It turns out that the rare-gas core positron-annihilation characteristics are extremely sensitive to the change of lattice constant (see column 10 of Table I); this could be experimentally verified in alkali metals, which have a high coefficient of thermal expansion[29] and where the difference in the rare-gas positron-annihilation rate between 4 K and room temperature should amount even to about 10%. Two-dimensional ACPAR experiments in the [110] direction would be especially desirable as they make it possible to isolate the core contribution in some momentum regions.[3]

Further, in some metals it is very important to include the correlation potential V_{corr} into the calculation of the positron wave function. The influence of V_{corr} in the rare-gas core annihilation rate is more pronounced in simple and noble metals and in Zn and Cd (9–16 %) than in 3*d* and 4*d* metals (cf. Table II, columns 5 and 7, Table III, columns 6 and 8). It is also advisable to use the electronic configurations corresponding to a solid[27,28] rather than the atomic configurations; the differences in resulting the rare-gas core annihilation rate may be as high as 7% (see column 5 in Table III). As the contribution of itinerant (valence) electrons to the annihilation rate displays behavior opposite to the change of electronic configuration, the differences in total annihilation rates are not so pronounced (column 10 in Table III). The corresponding ratios r_c^α and r^α (α is 0 or "corr") characterizing the changes in λ_c^α and λ^α with electron-positron correlation effects included behave similarly as r_c^{IPM} and r^{IPM} from Table III, as it may be checked by comparison of columns 5, 7, 9, and 10 of Table II with columns 6, 8, 11, and 12 of Table III, respectively.

The influence of the exchange-correlation potential employed in the calculations may also be appreciable (see column 7 in Table I); the differences in the rare-gas core

annihilation rates may reach even about 7%, if Hedin-Lundqvist or Slater exchange correlation is used. Relativistic effects become important in heavier elements (column 9 in Table I).

We have not found big differences in the rare-gas core positron-annihilation characteristics calculated with the positron wave function determined from the condition of the zero logarithmic derivative at the Wigner-Seitz radius or with a simple APW positron wave function.

A comparison of the calculated total annihilation rates with experimental data for 23 metals shows that the present approach using the solid-state electronic configurations with $V_{\rm corr}$ in the positron wave function included describes the experimental data fairly well and rather better than the treatment of Jensen.[6] This is probably also true in the case of the rare-gas core positron-annihilation characteristics. It may be expected that the application of the self-consistent crystal potential in the construction of electron and positron wave functions would bring even better agreement of calculated and experimental total annihilation rates—this was, however, not the subject of the present paper, and it is left for future investigations.

In conclusion, we may summarize that the calculation of rare-gas core positron-annihilation characteristics must be done equally well as the calculation of the contribution of itinerant electrons,[11,26] especially if one intends to draw some reliable quantitative conclusions from the comparison of theoretical and experimental results. Further experimental information concerning positron annihilation with rare-gas core electrons would be highly desirable.

[1]For a review of ACPAR studies, see, e.g., R. N. West, *Positron Studies of Condensed Matter* (Taylor & Francis, London, 1974); S. Berko, in *Positron Solid State Physics,* edited by W. Brandt and A. Dupasquier (North-Holland, Amsterdam, 1983), p. 64; S. Berko, in *Momentum Densities,* edited by R. N. Silver and P. E. Sokol (Plenum, New York, 1989), p. 273. Positron dynamics in solids is reviewed by W. Brandt, in *Positron Solid State Physics,* edited by W. Brandt and A. Dupasquier (North-Holland, Amsterdam, 1983), p. 1.

[2]M. Šob, Solid State commun. **53**, 249 (1985); *ibid.* **53**, 255 (1985); in *Positron Annihilation,* edited by P. C. Jain, R. M. Singru, and K. P. Gopinathan (World Scientific, Singapore, 1985), p. 104.

[3]L. Oberli, A. A. Manuel, R. Sachot, P. Descouts, and M. Peter, Phys. Rev. B **31**, 6104 (1985).

[4]A. Baranowski and E. Debowska, Appl. Phys. A **51**, 23 (1990).

[5]B. Chakraborty, in *Positron Annihilation,* edited by P. G. Coleman, S. C. Sharma, and L. M. Diana (North-Holland, Amsterdam, 1982), p. 207.

[6]M. J. Puska and R. M. Nieminen, J. Phys. F **13**, 333 (1983); K. O. Jensen, J. Phys. Condens. Matter **1**, 10 595 (1989).

[7]S. Daniuk, G. Kontrym-Sznajd, J. Majsnerowski, M. Šob, and H. Stachowiak, J. Phys. Condens. Matter **1**, 6321 (1989); G. Kontrym-Sznajd and J. Majsnerowski (unpublished).

[8]M. Šob, in *Positron Annihilation,* edited by L. Dorikens-Vanpraet, M. Dorikens, and D. Segers (World Scientific, Singapore, 1989), p. 131, and references therein.

[9]J. Mader, S. Berko, H. Krakauer, and A. Bansil, Phys. Rev. Lett. **18**, 1232 (1976); R. P. Gupta and R. W. Siegel, Phys. Rev. B **22**, 4572 (1980).

[10]P. E. Mijnarends and R. M. Singru, Phys. Rev. B **19**, 6038 (1979).

[11]H. Sormann and M. Šob, Phys. Rev. B **41**, 10 529 (1990).

[12]J. Arponen and E. Pajanne, Ann. Phys. **121**, 343 (1979); in *Positron Annihilation,* edited by P. C. Jain, R. M. Singru, and K. P. Gopinathan (World Scientific, Singapore, 1985), p. 21, and references therein. The density dependence of the total annihilation rates and correlation potentials obtained by Arponen and Pajanne was parametrized by E. Boroński and R. M. Nieminen, Phys. Rev. B **34**, 3820 (1986).

[13]A. Rubaszek and H. Stachowiak, Phys. Status Solidi B **124**, 159 (1984); Phys. Rev. B **30**, 2490 (1984); *ibid.* **38**, 3846 (1988), and references therein.

[14]H. Sormann and W. Puff, in *Positron Annihilation,* edited by P. C. Jain, R. M. Singru, and K. P. Gopinathan (World Scientific, Singapore, 1985), p. 161; H. Sormann, Phys. Status Solidi B **142**, K45 (1987).

[15]M. Šob, in *Proceedings of the 8th Annual International Symposium on the Electronic Structure of Metals and Alloys,* edited by P. Ziesche (Technische Universität, Dresden, 1978), p. 170; J. Phys. F **12**, 571 (1982).

[16]A. K. Singh, A. A. Manuel, T. Jarlborg, Y. Mathys, E. Walker, and M. Peter, Helv. Phys. Acta **59**, 410 (1986); M. Matsumoto and S. Wakoh, J. Phys. Soc. Jpn. **56**, 3566 (1987); Physica B **149**, 57 (1988).

[17]S. Daniuk, G. Kontrym-Sznajd, J. Mayers, A. Rubaszek, H. Stachowiak, P. A. Walters, and R. N. West, in *Positron Annihilation,* edited by P. C. Jain, R. M. Singru, and K. P. Gopinathan (World Scientific, Singapore, 1985), p. 43; S. Daniuk, G. Kontrym-Sznajd, A. Rubaszek, H. Stachowiak, J. Mayers, P. A. Walters, and R. N. West, J. Phys. F **17**, 1365 (1987). Present interpretation of parameter $X_{\mathbf{k}j}=\sqrt{E_{\mathbf{k}j}/E_F}$ differs from the one proposed by Daniuk *et al.* who employed the local kinetic energies, i.e., $X_{\mathbf{k}j}(\mathbf{r})=\sqrt{[E_{\mathbf{k}j}-V(\mathbf{r})]/[E_F-V(\mathbf{r})]}$, where $V(\mathbf{r})$ was the crystal potential.

[18]T. Jarlborg and A. K. Singh, Phys. Rev. B **36**, 4660 (1987).

[19]R. M. Nieminen and M. Manninen, Solid State Commun. **15**, 403 (1974); R. M. Nieminen and M. J. Puska, Phys. Rev. Lett. **50**, 281 (1983); A. P. Brown, A. B. Walker, and R. N. West, J. Phys. F **17**, 2491 (1987); A. P. Brown, K. O. Jensen, and A. B. Walker, *ibid.* **18**, 1141 (1988).

[20]A. Rubaszek and J. Lach, J. Phys. Condens. Matter **1**, 9243 (1989).

[21]S. Kahana, Phys. Rev. **129**, 1622 (1963).

[22]S. Daniuk, J. Phys. Condens. Matter **1**, 5561 (1989), and references therein.

[23]F. Herman and S. Skillman, *Atomic Structure Calculations* (Prentice-Hall, Englewood Cliffs, NJ, 1963).

[24]D. A. Liberman, D. T. Cromer, and J. T. Waber, Comput. Phys. Commun. **2**, 107 (1971).

[25]L. F. Mattheiss, Phys. Rev. **134**, A970 (1969).

[26]H. Sormann (unpublished).

[27]O. K. Andersen, O. Jepsen, and D. Glötzel, in *Highlights of*

Condensed Matter Theory, edited by F. Bassani, F. Fumi, and M. Tosi (North-Holland, Amsterdam, 1985), p. 59.
[28]D. A. Papaconstantopoulos, *Handbook of the Band Structure of Elemental Solids* (Plenum, New York, 1986).
[29]S. I. Novikova, *Teplovoye Rasshireniye Tverdych Tel* (Nauka, Moscow, 1974), p. 98.
[30]A. Seeger, F. Banhart, and W. Bauer, in *Positron Annihilation,* edited by L. Dorikens-Vanpraet, M. Dorikens, and D. Segers (World Scientific, Singapore, 1989), p. 275.
[31]D. O. Welch and K. G. Lynn, Phys. Status Solidi A **77**, 277 (1976).